Materials Science in Semiconductor Processing 72 (2017) 4–8

Contents lists available at ScienceDirect

Materials Science in Semiconductor Processing

journal homepage: www.elsevier.com/locate/mssp

Optical properties of thermally evaporated In_2S_3 thin films measured using photoacoustic spectroscopy

S. Rasool[a], K. Saritha[a], K.T. Ramakrishna Reddy[a,*], K. Raveendranath Reddy[b], L. Bychto[c], A. Patryn[c], M. Maliński[c], M.S. Tivanov[d], V.F. Gremenok[e]

[a] Solar Photovoltaic laboratory, Department of Physics, Sri Venkateswara University, Tirupati 517 502, Andhra Pradesh, India
[b] Department of Physics, Sri Govindaraja Swamy Arts College, Tirupati 517502, Andhra Pradesh, India
[c] Department of Electronics & Computer Sciences, Koszalin University of Technology, Koszalin 75-453, Poland
[d] Department of Energy Physics, Belarusian State University, Nezavisimosti 4 av., 220030 Minsk, Belarus
[e] Scientific and Practical Materials Research Centre, National Academy of Sciences, 220072 Minsk, Belarus

ARTICLE INFO

Keywords:
Thermal evaporation
In_2S_3
Thin films
GIXD
SEM
Photoacoustic spectroscopy
Optical properties

ABSTRACT

In_2S_3 is a III-VI group semiconductor with n-type conductivity and a wide band gap energy, which can be suitable as a buffer layer alternative to CdS in thin film solar cell fabrication. In the present study, In_2S_3 thin films were grown on glass substrates by the thermal evaporation method at a constant substrate temperature of 200 °C. The deposited layers were post annealed in vacuum in the temperature range of 200–300 °C for 1 h. The grazing incident X-ray diffraction and scanning electron microscopy studies revealed polycrystalline nature of the layers with a good surface morphology. The optical properties of these annealed layers were investigated by using photoacoustic spectroscopy and independently by using conventional optical transmission spectroscopy. The photoacoustic spectra of In_2S_3 films showed a sharp fall in the photoacoustic signal at photon energies that increased from 1.95 to 2.74 eV with increasing annealing temperature, which corresponds to the band gap energy of corresponding films. The band gap energy and the refractive index values calculated by using photoacoustic spectra are in good agreement with that determined from transmission spectra.

1. Introduction

CdS thin films are widely used as buffer layer in Cu(In,Ga)Se_2 and CdTe-based heterojunction thin film solar cells and play a vital role in enhancing the efficiency upto 20% [1]. Since Cd is a toxic material and it can cause severe damage to environment on large scale production, the alternative materials are of a great interest for researchers. In this context, In_2S_3 is an important alternative to CdS in Cu(In,Ga)Se_2 and Cu_2ZnSnS_4 thin film solar cells [2,3], because of its eco-friendly nature with wide energy band gap and photoconductive behaviour [4]. It is a n-conductivity type direct band gap semiconductor and has a high quantum conversion efficiency (70–80%) in the visible region [5]. Recently, 16.4% of conversion efficiency has been achieved by using In_2S_3 as a buffer layer in Cu(In,Ga)Se_2 based solar cells, which is close to that achieved using CdS as the buffer layer [6]. Till now, various deposition techniques have been used to prepare In_2S_3 films, which showed significant impact on the behaviour of the grown films. The reported band gap values of In_2S_3 films were varied from 2.0 to 3.3 eV [7,8] depending on the growth techniques and deposition conditions. Barreau et al. [9] reported a band gap of 2.80 eV for n-type In_2S_3 layers grown by physical vapour deposition in oxygen atmosphere. The chemical bath deposited films showed band gap in the range of 2.0–2.8 eV [10], by using atomic layer chemical vapour deposition the obtained band gap is 2.7 eV [11], from thermal evaporation technique the obtained optical band gap values varied in the range of 2.0–2.2 eV [12], in the range of 2.46–2.73 eV from physical vapour deposition [13] and in the range of 2.0–2.8 eV from ultrasonically sprayed layers [14].

In the present study, In_2S_3 films were grown by vacuum thermal evaporation technique at a substrate temperature of 200 °C and annealed in vacuum in the temperature range from 200 °C to 300 °C. The optical properties of the In_2S_3 films were evaluated by using photoacoustic (PA) spectroscopy and compared with the results of optical transmission spectroscopy. The PA spectroscopy is a non-destructive and sensitive technique that gives direct information related to the optical and thermal properties of semiconductors [15]. The PA spectroscopy technique is a very useful tool for effective study of semiconductor films either amorphous or polycrystalline in nature where spectroscopic methods fail, for example, in the case of semiconductor

* Corresponding author.
E-mail addresses: rasool265@gmail.com (S. Rasool), sarayuphysics@gmail.com (K. Saritha), ktrkreddy@gmail.com (K.T.R. Reddy).

http://dx.doi.org/10.1016/j.mssp.2017.09.009
Received 30 June 2017; Received in revised form 3 September 2017; Accepted 9 September 2017

films formed on an opaque substrates. There are several advantages of the PA spectroscopy for the optical analysis: it is little affected by the surface morphology and roughness; it detects a signal, which is directly proportional to the generated thermal energy; there are no special demands regarding sample preparation; it exhibits smaller influence of the interference effects on the measured spectra than in the transmission spectroscopy. However, there are only few available reports on photothermal studies of In_2S_3 films. Earlier, the thermal and optical properties of Al-doped In_2S_3 samples were studied with the photothermal deflection (PD) spectroscopy and reported [16]. In this paper, the PA spectroscopy has been used as an investigation tool for determining the optical characteristics of the In_2S_3 films. Very few articles are available on PA spectroscopic studies of In_2S_3 material in the form of single crystal [17] and nano flakes/dendrites type [18], but not in polycrystalline thin film form. Therefore, it is the first report on optical properties of thermally evaporated In_2S_3 films measured by PA spectroscopy.

2. Experimental details

In_2S_3 films were deposited by thermal evaporation technique (Hind Hi Vac box coater BC-300) using In_2S_3 powder (Sigma Aldrich, 99.999% purity) as a source material. The films were deposited on soda lime glass substrates at a constant temperature (T_s) of 200 °C by maintaining a source to substrate distance of 14 cm and deposition rate of 15 Å/sec, while the thickness of the films was maintained as ≈ 200 nm as measured by quartz crystal thickness monitor. The as-grown films were annealed in vacuum (2×10^{-2} mbar) at various temperatures (T_a) in the range of 200–300 °C for 60 min by using a two zone tabular furnace. The structural characteristics of the samples were analyzed by using an Ultima IV X-ray diffractometer in the grazing incidence diffraction geometry (GIXD) at 1 degree of incident X-rays with Cu Kα radiation source (λ = 1.5406 Å). The surface morphology and cross-sectional view of the films were investigated by using a Hitachi S-806 scanning electron microscope (SEM). The optical properties of the films were measured by using a high-resolution PA spectrometer and by using a Photon RT spectrophotometer (Essent Optics).

PA spectroscopy is the application of the photoacoustic effect for spectroscopic purposes. The basic principle of photoacoustic effect is the generation of acoustic signal, when a material is illuminated with modulated or pulsed light. The PA spectroscopy set-up used in this work is presented in Fig. 1. The light emitted by a Xenon lamp of 300 W light intensity is introduced into an OMNI-300 grating monochromator with the operation range of 600–2400 nm. The monochromated light is modulated by a Standford Research SR540 mechanical chopper and falls on a homemade photoacoustic cell, which contains the sample and a microphone (40AP type condenser microphone with a 26AK preamplifier by G.R.A.S.). The amplitude and phase of the photoacoustic signal (PAS) coming from the sample is measured in the form of sound and vibration by a Standford Research SR830 lock-in amplifier. The whole system is controlled by a computer with the software written in LAB view. Further, two types of measurements can be performed for characterizing the sample in PA spectroscopy: (i) (PAS) versus

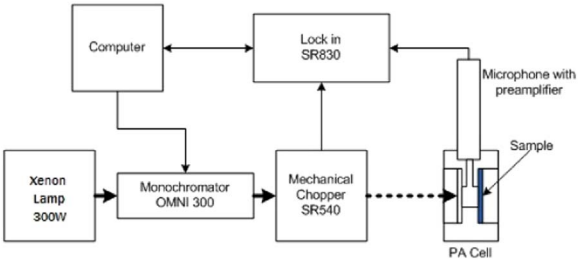

Fig. 1. Experimental set-up of PA spectroscopy measurement unit.

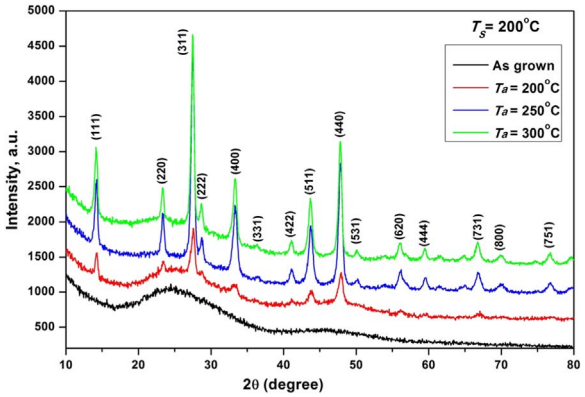

Fig. 2. GIXD patterns of In_2S_3 layers.

wavelength of the light at constant modulation frequency and (ii) PAS versus frequency of modulation at constant wavelength. From the first type of measurement, one can obtain the optical parameters of the sample when the thermal parameters are known, whereas in the latter case, the thermal parameters of the sample can be obtained.

3. Results and discussions

The as-grown In_2S_3 thin films were found to be homogeneous, pin hole free, appeared dark reddish yellow in colour and well adherent to the substrate surface. After the deposition and annealing process, the thickness of the films was ≈ 200 nm.

3.1. Structural analysis

Fig. 2 shows the GIXD patterns of the as-grown and thermally annealed (at three different temperatures 200, 250 and 300 °C) In_2S_3 films. The GIXD pattern revealed that the as-grown films possess amorphous nature, which might be due to insufficient thermal energy to induce crystallization. Zhong et al. [19] also reported the similar behaviour in thermally evaporated In_2S_3 layers deposited at different substrate temperatures (upto 500 °C). Annealing of the as-grown layers triggered the crystallization in the films. The annealed layers exhibited polycrystalline nature with (311) plane as preferred orientation along with the existence of other peaks corresponding to (111), (220), (222), (400), (331), (422), (511), (440), (531), (620), (444), (731), (800) and (751) planes. The presence of these peaks confirmed the existence of cubic structured β-In_2S_3 phase and matches with the JCPDS data file no. 65-0459. Further, it was observed from the figure that the intensity of the dominant diffraction peak increases with annealing temperature, indicating that the crystal quality of the films was improved. This was attributed to the coalescence induced grain growth during the annealing process [20]. Rao et al. [21] also noticed a similar observation, where the crystallinity of thermally evaporated In_2S_3 films increased with the increase of annealing temperature.

The crystallographic parameters like crystallite size (D) and internal lattice strain (ε) were calculated for annealed In_2S_3 films using the following relations and the obtained values were tabulated in Table 1.

The inter-planar spacing (d) was calculated using the Bragg's diffraction law:

Table 1
The crystallographic parameters of the annealed In_2S_3 thin films.

Annealing temperature (°C)	2θ (°)	β (rad)	d-spacing (nm)	D (nm)	ε ($\times 10^{-3}$)
200	27.55	0.0103	0.323	28	10.5
250	27.50	0.0092	0.324	32	9.3
300	27.45	0.0085	0.324	36	8.7

$$n\lambda = 2d \sin\theta, \quad (1)$$

where n is the integer, λ is the wavelength of incident radiation, and θ is the Bragg's angle.

The crystallite size was evaluated using the Debye-Scherrer formula [22]:

$$D = \frac{0.94\lambda}{\beta \cos\theta}, \quad (2)$$

where β is the full width at half maximum of the predominant peak.

The lattice strain in the films was calculated by using the following relation [23]:

$$\varepsilon = \frac{\beta}{4 \tan\theta}. \quad (3)$$

From the above table, it is observed that the crystallite size slightly increased, whereas the lattice strain decreased with the increase of annealing temperature, which indicates the improvement in the crystallinity of the films.

3.2. Surface morphology

The top-view and cross-sectional SEM micrographs of the In_2S_3 films are shown in Fig. 3. According to GIXD results (see above), the as-grown films have amorphous nature. The surface morphology observed in Fig. 3(a) corresponds to clusters of material. The grain structure begins to appear only after annealing (Fig. 3(b) and (c)). It is obvious from SEM images that the crystallinity of the films increases with increasing annealing temperature, which supports the results obtained from the GIXD analysis. At lower annealing temperatures the crystallites are very small and randomly distributed, while at T_a = 300 °C the crystallites are uniformly distributed over the substrate surface. Further, the films are uniform, homogeneous, free from defects and voids, and the grains are densely packed at this annealing temperature. This is mainly because during the process of annealing, recrystallization had occurred in the films, which enhanced the crystallite size [24]. This results in a significant improvement of the surface morphology.

3.3. Optical properties

The PA spectra were measured in the wavelength range of 400–900 nm at a constant frequency of modulation (f = 36 Hz). The obtained PA spectra were then calibrated with the signal from the glassy carbon as it is a commonly used in spectroscopy as the reference sample. For the analysis, all PA characteristics were normalized at 400 nm. The normalized PA spectra of In_2S_3 films are shown in Fig. 4 that demonstrates variation of the PA amplitude with the photon energy for the studied In_2S_3 films. All the PA spectra showed a sharp fall at photon energies that correspond to the band gap energy of the films. The steep increase of PAS indicates the direct type of the fundamental transitions in the films. The band gap energy, E_g can be obtained from PA spectra by using the relationship $(\alpha^*h\nu)^2 = A(E_g - h\nu)$, where α is the absorption coefficient. For small values of the optical absorption

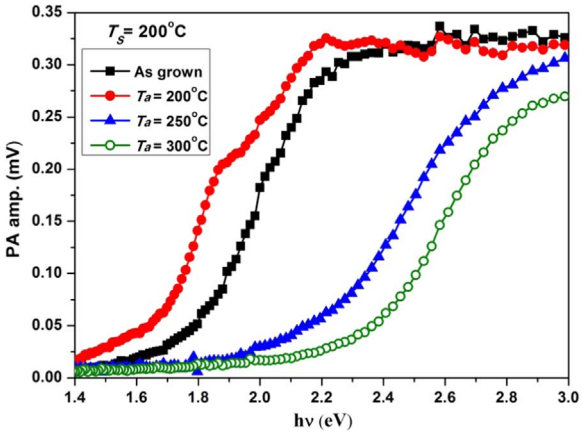

Fig. 4. Photoacoustic spectra of In_2S_3 films.

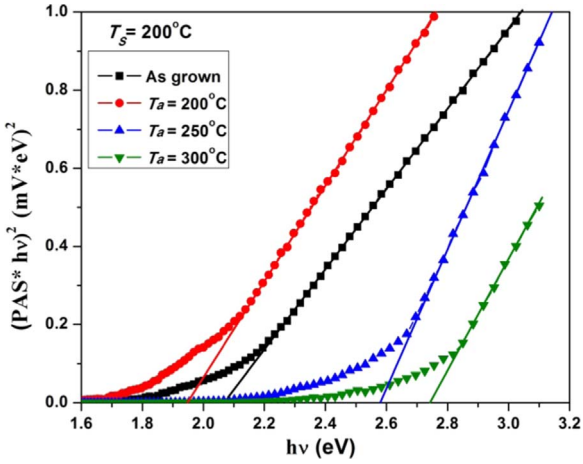

Fig. 5. Plot of $(PAS^*h\nu)^2$ versus (hν).

coefficient, $(\alpha^*h\nu) \propto (PAS^*h\nu)$ [25,26]. Therefore, value of E_g can be determined by the extrapolation of the linear part of the $(PAS^*h\nu)^2 - h\nu$ plot onto the hν axis. It can be seen from Fig. 5 that the energy band gap varied from 1.95 to 2.74 eV with the change of annealing temperature. The observed decrease of the energy band gap with annealing at low temperature and its subsequent increase at higher annealing temperatures has been also reported previously [27,28]. The decrease of the energy band gap could be determined by an increase in the structural order induced during the structural change from the amorphous to the crystalline stable phase [28]. At higher temperatures, the energy band gap increases with increasing annealing temperature, which might be due to the change in the crystallinity and lattice defects present in the films [29].

The refractive index (n) for the In_2S_3 films was calculated from PA spectra using the Herve-Vandamme formula [30]

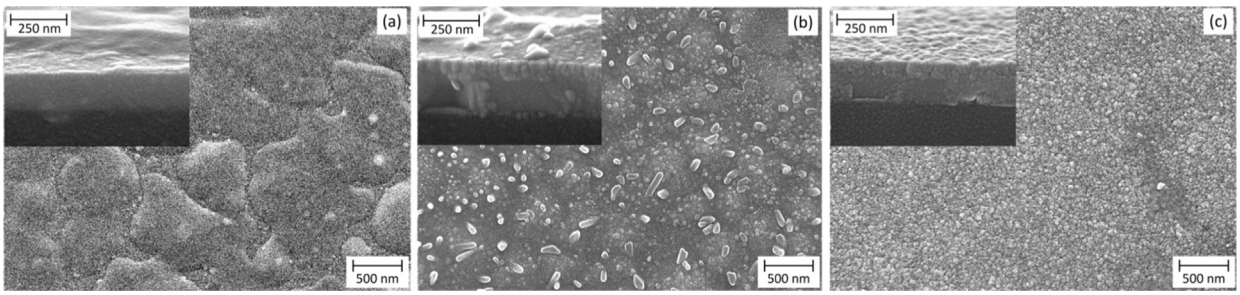

Fig. 3. Top-view and cross-sectional (insets) SEM images of In_2S_3 thin films: (a) as-grown; annealed at (b) T_a = 250 °C and (c) T_a = 300 °C.

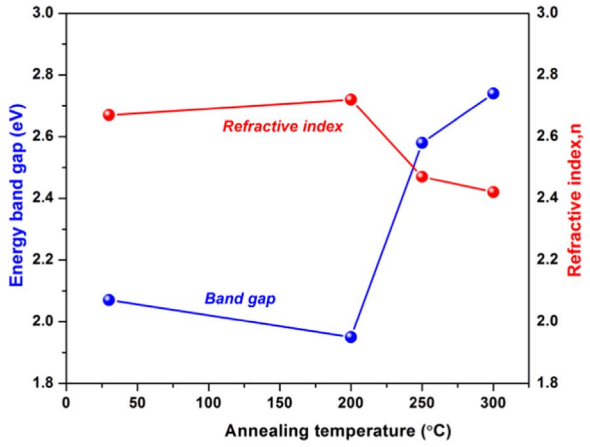

Fig. 6. The variation of band gap energy and refractive index with annealing temperature.

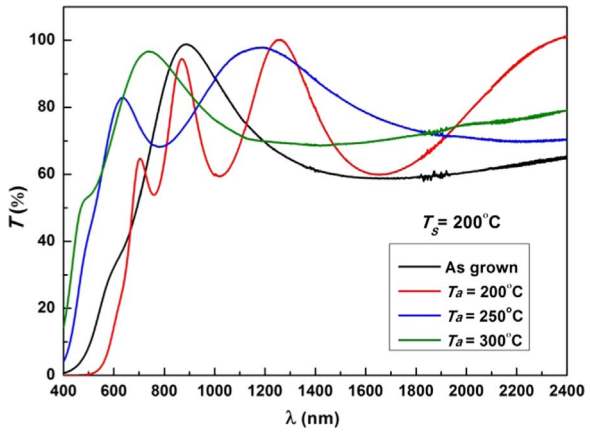

Fig. 7. Transmittance versus wavelength spectra for In_2S_3 films.

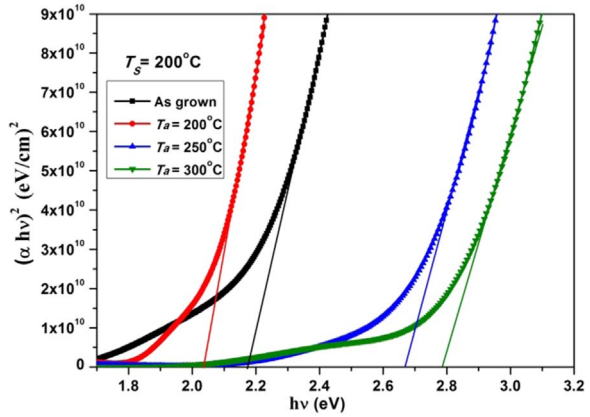

Fig. 8. Tauc plots for In_2S_3 films.

$$n^2 = 1 + \left(\frac{A}{E_g + B}\right)^2, \tag{4}$$

where A and B are constants equal to 13.6 eV and 3.4 eV, respectively. Fig. 6 demonstrates that the refractive index is varied with annealing temperature in the range of 2.72–2.42. This variation in refractive index can be attributed to the change in the strain and packing density of the layers [31]. El-Nahass et al. [32] also reported that refractive index decreased with increase of annealing temperature of In_2S_3 thin films deposited by the thermal evaporation technique. The low refractive index indicates high transmittance of light through the film.

The band gap energy of In_2S_3 films was also evaluated from the optical transmittance spectra using the Tauc plots. The transmission (T) versus wavelength (λ) spectra were measured in the wavelength range of 300–2500 nm (Fig. 7). Using the T versus λ data, the optical absorption coefficient, α was calculated for a typical film thickness of 200 nm. Fig. 8 shows that the optical band gap energy evaluated from the Tauc plots varies in the range of 2.03–2.78 eV for films annealed at different temperatures. The obtained values of band gap energy are nearly in agreement with the values of band gap energy determined from the PA measurements.

Also, the refractive index of In_2S_3 films was calculated through the transmission maxima, T_M and minima, T_m of the envelopes of the transmission spectra, by using the Swanepoel method [33]:

$$n^2 = [N + (N^2 - s^2)^{1/2}] \tag{5}$$

$$N = 2s\frac{T_M - T_m}{T_M T_m} + \left(\frac{s^2 + 1}{2}\right), \tag{6}$$

where $s = 1.5$ is the refractive index of the substrate (glass). The refractive index values were obtained as 2.70, 2.75, 2.43 and 2.39 for the as-grown films and the films annealed at 200, 250 and 300 °C, respectively. These values were nearly in agreement with the refractive index values determined from the PA measurements.

4. Conclusion

In_2S_3 films were deposited on glass substrates using thermal evaporation technique at a constant substrate temperature of 200 °C with subsequent annealing at 200, 250 and 300 °C. X-ray diffraction analysis revealed the amorphous state of the as-grown films, whereas annealing gives rise to an improvement of crystallinity with formation of the preferred (311) orientation. The optical properties of In_2S_3 thin films were analyzed using photoacoustic spectroscopy and optical transmission spectroscopy. It was found that computation of the band gap energy and the refractive index values from photoacoustic or optical transmission spectra yields similar results. Thus, the photoacoustic spectroscopy can be applied for reliable determination of optical properties of semiconductor layers, which is extremely important in cases, when transmission spectroscopy is impossible. From the present analysis, it is inferred that the samples annealed at 300 °C showed a good crystallinity, uniform surface morphology and band gap energy of 2.74 eV. Hence, this temperature might be considered as appropriate for formation of In_2S_3 buffer layers in thin film solar cells.

Acknowledgements

The authors, Prof. K.T. Ramakrishna Reddy and Prof. V. Gremenok wish to acknowledge the Department of Science & Technology, Government of India (Grant no. DST/INT/IND-BLR/P-9/2014) and the Belarusian Republican Foundation for Fundamental Research (Grant No. T15-IND-001), Republic of Belarus respectively for the financial support in the form of joint research project to carry out this work.

References

[1] O. Poncelet, R. Kotipalli, B. Vermang, A. Macleod, L.A. Francis, D. Flandre, Optimization of rear reflectance in ultra-thin CIGS solar cells towards > 20% efficiency, Sol. Energy 146 (2017) 443.
[2] S. Buecheler, D. Corica, D. Guettler, A. Chirila, R. Verma, U. Muller, T.P. Niesen, J. Palm, A.N. Tiwari, Ultrasonically sprayed indium sulfide buffer layers for Cu(In,Ga)(S,Se)$_2$ thin film solar cells, Thin Solid Films 517 (2009) 2312.
[3] L. Lin, Ji Yu, Sh Cheng, P. Lu, Yu Lai, S. Lin, P. Zhao, Band alignment at the In_2S_3/Cu_2ZnSnS_4 heterojunction interface investigated by X-ray photoemission spectroscopy, Appl. Phys. A 116 (2014) 2173.
[4] Y.J. Hsiao, C.H. Lu, L.W. Ji, T.H. Meen, Y.L. Chen, H.P. Chi, Characterization of photovoltaics with In_2S_3 nano flakes/p-Si heterojunction, Nanoscale Res. Lett. 9 (2014) 32.
[5] C.D. Lokhande, A. Ennoui, P.S. Patil, M. Giersig, K. Diesner, M. Muller, H. Tributsch, Chemical bath deposition of indium sulfide thin films: preparation and

characterization, Thin Solid Films 340 (1999) 18.
[6] D. Abou-Ras, G. Kostorz, D. Hariskos, R. Menner, M. Powalla, S. Schorr, A.N. Tiwari, Structural and chemical analyses of sputtered In_xS_y buffer layers in Cu(In,Ga)Se_2 thin-film solar cells, Thin Solid Films 517 (2009) 2792.
[7] J. George, K.S. Joseph, B. Pradeep, T.I. Palson, Reactively evaporated films of indium sulfide, Phys. Status Solidi A 106 (1988) 123.
[8] E.B. Yousfi, B. Weiberg, F. Donsanti, P. Cowache, D. Lincot, Atomic layer deposition of zinc oxide and indium sulfide layers for Cu(In,Ga)Se_2 thin-film solar cells, Thin Solid Films 387 (2001) 29.
[9] N. Barreau, J.C. Bemede, H.E.I. Maliki, S. Marsillac, X. Castel, J. Pinel, Recent studies on In_2S_3 containing oxygen thin films, Solid State Commun. 122 (2002) 445.
[10] I. Puspitasari, T.P. Gujar, K.-D. Jung, O.-S. Joo, Simple chemical method for nanoporous network of In_2S_3 platelets for buffer layer in CIS solar cells, J. Mater. Process. Technol. 201 (2008) 775.
[11] S. Spiering, D. Hariskos, M. Powalla, N. Naghavi, D. Lincot, Cd-free Cu(In,Ga)Se_2 thin-film solar modules with In_2S_3 buffer layer by ALCVD, Thin Solid Films 431 (2003) 359.
[12] A. Timouni, H. Bouzouita, M. Kanraz, B. Rezig, Fabrication and characterization of In_2S_3 thin films deposited by thermal evaporation technique, Thin Solid films 480 (2005) 124.
[13] J.F. Trigo, B. Asenjo, J. Herrero, M.T. Gutie'rrez, Optical characterization of In_2S_3, solar cell buffer layers grown by chemical bathand physical vapor deposition, Sol. Energy Mater. Sol. Cells 92 (2008) 1145.
[14] K. Emits, D. Bremaud, S. Buecheler, C.J. Hibberd, M. Kaelin, G. Khrypunov, U. Miiller, E. Mellikov, A.N. Tiwari, Characterization of ultrasonically sprayed In_xS_y buffer layers for Cu(In,Ga)Se_2 solar cells, Thin Solid Films 515 (2007) 6051.
[15] A.G. Bell, On the production and reproduction of sound by light, Am. J. Sci. 20 (1880) 305.
[16] F. Saadallah, N. Jebbari, N. Kammoun, N. Yacoubi, Optical and thermal properties of In2S3, Int. J. Photo. (2011) (Article ID 734574).
[17] W.T. Kim, W.S. Sub Lee, C.S. Chung, C.D. Kim, Optical properties of In_2S_3: Co^{2+} single crystals, J. Appl. Phys. 63 (1988) 5472.
[18] Ch.R. Patra, S. Patra, A. Gabashvili, Yi Mastai, Yu Koltypin, A. Gedanken, V. Palchik, M.A. Slifkin, A microwave route for the synthesis of nanoflakes and dendrites-type β- In_2S_3 and their characterization, J. Nanosci. Nanotechnol. 6 (2006) 845.
[19] Z.Y. Zhong, E.S. Cho, S.J. Kwon, Effect of substrate temperatures on evaporated In_2S_3 thin film buffer layers for Cu(In,Ga)Se_2 solar cells, Thin Solid Films 547 (2013) 22.
[20] K.L. Chopra, Thin Film Phenomena, McGraw-Hill, New York, 1969, p. 163.
[21] P. Rao, S. Kumar, Growth of stoichiometric indium sulfide films by thermal evaporation: influence of vacuum annealing on structural and physical properties, Thin Solid Films 524 (2012) 93.
[22] B.E. Warren, X-ray Diffraction, Dover, New York, 1990, p. 253.
[23] A. Purohit, S. Chander, S.P. Nehra, M.S. Dhaka, Effect of air annealing on structural, optical, morphological, and electrical properties of thermally evaporated CdSe thin films, Phys. E 69 (2015) 342.
[24] D.H. Shin, L. Larina, K.H. Yoon, B.T.A. Shin, Fabrication of Cu(In,Ga)Se_2 solar cell with ZnS/CdS double layer as an alternative buffer, Curr. Appl. Phys. 10 (2010) 5142.
[25] M.L. Albor-Aguilera, M.A. González-Trujillo, A. Cruz-Orea, M. Tufiño-Veláquez, Thermal and optical properties of polycrystalline CdS thin films deposited by the gradient recrystallization and growth (GREG) technique using photoacoustic methods, Thin Solid Films 517 (2009) 2335.
[26] S.A. Mayén-Hernández, G. Torres-Delgado, R. Castanedo-Pérez, M. Gutiérrez-Villarreal, A. Cruz-Orea, J.G. Mendoza-Álvarez, O. Zelaya-Ángel, Optical and structural properties of ZnO + Zn_2TiO_4 thin films prepared by the sol-gel method, J. Mater. Sci.: Mater. Electron. 18 (2007) 1127.
[27] M.G. Sandoval-Paz, M. Sotelo-Lerma, J.J. Valenzuela-Ja´uregui, M. Flores-Acosta, R. Ramirez-Bon, Structural and optical studies on thermal-annealed In_2S_3 films prepared by the chemical bath deposition technique, Thin Solid Films 472 (2005) 5.
[28] H. Izadneshan, V.F. Gremenok, Influence of annealing on the optical parameters of In_2S_3 thin films produced by thermal evaporation, J. Appl. Spectrosc. 81 (2014) 293.
[29] N. Revathi, P. Prathap, R.W. Miles, K.T. Ramakrishna Reddy, Annealing effect on the physical properties of evaporated In_2S_3 films, Sol. Energy Mater. Sol. Cells 94 (2010) 1487.
[30] S.P. Nehra, S. Chander, A. Sharma, M.S. Dhaka, Effect of thermal annealing on physical properties of vacuum evaporated In_2S_3 buffer layer for eco-friendly photovoltaic applications, Mater. Sci. Semicond. Process. 40 (2015) 26.
[31] V. Gupta, A. Mansingh, Influence of post deposition annealing on the structural and optical properties of sputtered zinc oxide films, J. Appl. Phys. 80 (1996) 1063.
[32] M.M. El-Nahass, B.A. Khalifa, H.S. Soliman, M.A.M. Seyam, Crystal structure and optical absorption investigation on β-In_2S_3 thin films, Thin Solid Films 515 (2006) 1796.
[33] R. Swanepoel, Determination of the thickness and optical constants of amorphous silicon, J. Phys. E: Sci. Instrum. 16 (1983) 1214.